Atmosphere **2013**, *4*, 272-298; doi:10.3390/atmos4030272

OPEN ACCESS

atmosphere

ISSN 2073-4433

www.mdpi.com/journal/atmosphere

Article

On the Current and Future Dry Spell Characteristics over Africa

Bessam Bouagila * and Laxmi Sushama

Centre ESCER (Étude et Simulation du Climat à l'Échelle Régionale), University of Quebec at Montreal, 201-President-Kennedy, Montreal, QC H3C3P8, Canada

* Author to whom correspondence should be addressed; E-Mail: bessam@sca.uqam.ca; Tel.: +1-514-987-3000 (ext. 2414); Fax: +1-514-987-6853.

Received: 24 June 2013; in revised form: 30 July 2013 / Accepted: 24 August 2013 / Published: 9 September 2013

Abstract: Changes in precipitation frequency and intensity distribution over Africa will have a direct impact on dry spells and, therefore, will affect various climate sensitive sectors. In this study, the ability of the fifth generation of the Canadian Regional Climate Model (CRCM5) in simulating annual and seasonal dry spell characteristics is assessed for four precipitation thresholds (0.5 mm, 1 mm, 2 mm and 3 mm) over Africa. The dry spell characteristics considered are the number of dry days, number of dry spells and five-year return levels of maximum dry spell durations. The performance errors are assessed by comparing ERA-Interim driven CRCM5 with the Global Precipitation Climatology Project (GPCP) dataset, for the common 1997–2008 period. Lateral boundary forcing errors, *i.e.*, errors in the CRCM5 simulation created by errors in the driving Canadian Earth System model (CanESM2) data—as well as the added value—of CRCM5 over CanESM2 are also assessed for the current climate. This is followed by an assessment of projected changes to dry spell characteristics for two future climates (2041–2070 and 2071–2100) simulated by both CRCM5 driven by CanESM2 and CanESM2 itself, for Representative Concentration Pathway (RCP) 4.5. Results suggest that CRCM5 driven by ERA-Interim has a tendency to overestimate the annual mean number of dry days and the five-year return level of the maximum dry spell duration in a majority of the regions while it slightly underestimates the number of dry spells. In general, the CRCM5 performance errors associated with the annual and seasonal dry spell characteristics are found to be larger in magnitude compared to the lateral boundary forcing errors. Projected changes to the dry spell characteristics for the 2041–2070 and 2071–2100 periods, with respect to the 1981–2010 period suggests significant changes in the tropics, with the mean number of dry days and the five-year

return levels of maximum dry spell duration increasing, while the mean number of dry spell days decreases.

Keywords: dry spell characteristics; regional climate model; Africa; climate change

1. Introduction

According to the Intergovernmental Panel on Climate Change (IPCC) [1], Africa is one of the most vulnerable continents to climate change and climate variability. Global Climate Models (GCMs) participating in IPCC's fourth Assessment Report suggest warmer temperatures, in the range of 2–7 °C for Africa by the end of the 21st century. This warming is non-uniform, with the drier subtropical regions projected to experience warmer temperatures than the moist tropical region. As for precipitation, annual amounts are expected to decrease in parts of Africa above 20°N and below 25°S, while an increase is expected in the Horn of Africa. For regions such as Sahel and the Guinean coast, annual and seasonal mean precipitation show no clear signal [1].

Changes in precipitation frequency and intensity distribution can have an impact on dry and wet spells and, therefore, will affect various climate sensitive sectors, primarily agriculture. For most parts of Africa, agriculture is predominantly rain fed and thus, very vulnerable to changes in precipitation. The uneven seasonal distribution of precipitation can expose crops to a range of mild to severe intra-seasonal dry spells, which may affect the yield [2]. For example, for East Africa (Kenya-Uganda-Tanzania), Shongwe *et al.* [3] report a positive shift in the precipitation distribution, *i.e.*, an increase in high intensity precipitation events, by the end of the century for the two wet seasons (October–December and March–May) based on GCM projections. Their study also suggests less severe droughts for East Africa.

Several previous studies [4–6] have assessed projected changes to global precipitation characteristics using GCMs. Tebaldi *et al.* [6] studied projected changes to 10 indicators of climate extremes using an ensemble of nine GCMs according to a range of emission scenarios. Their study, despite the large spread in GCMs, showed on average a general decrease in the number of dry days (days with precipitation less than 1 mm) for the central east part of the tropics and an increase for the subtropics, over the African continent, for the A1B scenario. The large spread in GCM projections, particularly over Africa, is an indication of the challenges in simulating climate characteristics of the continent. In fact, climatic models still represent the main characteristics in and around Africa with significant errors such as excessive precipitation in the south, southward displacement of the Atlantic Inter-Tropical Convergence Zone (ITCZ), and insufficient upwelling near the Kalahari desert [1], making it difficult to assess the changes in future climate with confidence.

Though GCMs provide better simulations for the atmospheric general circulation at a larger scale, they do not offer required detail for regional and local assessment. This is particularly true for heterogeneous regions, with important variations of topography, vegetation, soils and coastlines [7]. Extreme events such as heavy precipitation are often not well-captured by GCMs. In fact, Sun *et al.* [8] showed that over land, most current GCMs overestimate light precipitation (1–10 mm/day) and underestimate heavy precipitation (>10 mm/day). Since precipitation processes occur at finer

resolution [9], the Regional Climate Model (RCM) is a more adequate tool for many regional impact and adaptation studies [10–14].

Although the use of RCMs over Africa is still in its infancy [15], efforts have been made to assess the main climatic features of Africa with regional models; Sun *et al.* [16,17] used RegCM2 from the National Center for Atmospheric Research to investigate precipitation over East Africa, while Patricola *et al.* [18] studied the dynamics of the West African Monsoon with the Weather Research and Forecasting (WRF) model, and Ibrahim *et al.* [19] used five RCMs for the same region. Joubert *et al.* [20] used the Division of Atmospheric Research Limited Area Model (DARLAM) from Commonwealth Scientific and Industrial Research Organisation, and Hudson *et al.* [21] used the Hadley Regional Climate Model (HadRM3H) to examine the climate of southern Africa.

In response to the vulnerability of Africa to climate change stated in the fourth Assessment Report of the IPCC [1], many recent international projects such as the Assessment of Impact and Adaptation to Climate Change (AIACC) [22], the Greater Horn of Africa Regional Model Intercomparison Project (AFRMIP) [23], the African Monsoon Multidisciplinary Analysis (AMMA) [24–26] and the West African Monsoon Modeling and Evaluation (WAMME) [27,28] have focused on the application of RCMs over Africa. The latest in the series of international projects, CORDEX [29] was initiated to evaluate and improve the ability of an ensemble of RCM simulations, including CRCM5 [30,31], over selected domains, such as Africa. CORDEX is also providing a standardized framework of Regional Climate Downscaling for improved regional climate change adaptation and impact assessment (http://wcrp.ipsl.jussieu.fr/cordex/about.html). Africa was selected as the first target region in order to improve simulation of key elements of current climate and then providing climate-change projections with various RCMs. Despite this recent increase in RCM application over Africa, study of extreme events is still very limited for the region [1].

So far, no studies on projected changes to dry spell characteristics over the African continent using RCMs are available. Such studies are required to aid develop adaptation strategies in the context of a changing climate. This article presents a thorough analysis of the annual and seasonal dry spell characteristics over Africa, as simulated by the fifth generation of the Canadian Regional Climate Model (CRCM5) in the current climate, and their projected changes for future periods. Projected changes based on the Canadian Earth System Model (CanESM2), which provides driving data at the CRCM5 lateral boundaries, are also investigated for the Representative Concentration Pathway (RCP) 4.5 scenario. The RCPs, which are based on simulations from a set of Integrated Assessment Models (IAMs), provide both concentration and emissions of radiatively important greenhouse gases emissions for several aerosols and their precursor species, and associated land cover change scenarios. In total, a set of four pathways—RCPs 2.6, 4.5, 6 and 8.5—were produced that lead to radiative forcing levels of 2.6, 4.5, 6 and 8.5 W/m^2 by the end of the century [32].

The paper is organized as follows: section two describes CRCM5 experimental configuration, observation datasets used and the methodology followed. Assessment of performance and boundary forcing errors and added value of CRCM5 are presented in section three, followed by assessment of projected changes to dry spell characteristics for two future periods (2041–2070 and 2071–2100) with respect to the current 1981–2010 period, for RCP 4.5 scenario. Summary and conclusions are presented in section four.

2. Model, Experimental Configuration, Datasets and Methods

2.1. Model and Experimental Configuration

The RCM considered in the study is CRCM5 [33], which is based on a limited-area version of the Global Environment Multiscale (GEM) model used for Numerical Weather Prediction (NWP) at Environment Canada [34,35]. GEM uses semi-Lagrangian transport and (quasi) fully implicit marching scheme. In its fully elastic non-hydrostatic formulation [36], GEM uses a vertical coordinate based on hydrostatic pressure [37]. The following GEM parameterisations are used for CRCM5: deep convection following Kain *et al.* [38], shallow convection based on a transient version of Kuo's scheme [39,40], large scale condensation [41], correlated-k solar and terrestrial radiations [42], subgridscale orographic gravity-wave drag [43], low-level orographic blocking [44], and turbulent kinetic energy closure in the planetary boundary layer and vertical diffusion [45–47]. In CRCM5, the usual GEM land-surface scheme has been replaced by CLASS version 3.4 [48] that allows a mosaic representation of land-surface types and a flexible number of soil layers in the vertical; in this article, 26 soil layers varying in thickness from 0.1 m at the surface to 5 m at the bottom are used.

A 150-year integration, spanning the 1951–2100 period on a 201 × 194 points grid (Figure 1a) covering the whole of Africa and the adjoining oceans at 45 km horizontal grid spacing and 56 levels in the vertical is considered in this paper. This integration performs dynamical downscaling of the CanESM2 simulation to produce climate projections at the regional scale. In this simulation, the Sea Surface Temperature (SST) is prescribed and corresponds to that of CanESM2. CanESM2 simulation grid has a horizontal resolution of 2.81° with 35 vertical layers (Figure 1b), and follows RCP 4.5 [32] scenario for the 2010–2100 period.

Though the CRCM5 simulation spans the 1951–2100 period, this study focuses on the current 1981–2010 and the future 2041–2070 and 2071–2100 30-year periods.

In addition, a validation experiment, *i.e.*, CRCM5 simulation forced at the lateral boundary by ERA-Interim [49,50] data from the European Centre for Medium-Range Weather Forecasts (ECMWF) for the 1984–2008 period is also considered. In this simulation, the prescribed SST follows ERA-Interim. According to IPCC, RCM simulations nested by reanalysis can reveal RCM 'performance errors' primarily due to the dynamics and physics of the regional model, and should precede any attempt to make climate-change projections [10]. Hereafter, the CRCM5 driven by ERA-Interim and CRCM driven by CanESM2 will be referred to as CRCM5_ERA_Interim and CRCM5_CanESM2, respectively.

2.2. Observational Data

The observed dry spell characteristics used for evaluating CRCM5 are derived from the Global Precipitation Climatology Project (GPCP) [51] 1 × 1° dataset (Figure 1c) covering 40°N to 40°S at three-hourly intervals. GPCP is based on geosynchronous satellite data and gauge measurements from the Global Precipitation Climatology Center (GPCC). The data set extends from October 1996 to present.

Figure 1. African simulation domain for (a) the fifth generation Canadian Regional Climate Model (CRCM5) at 0.44° horizontal resolution, with only every fifth grid box displayed. The dashed lines represent the 10 grid-point nesting zone and the dotted line represents the domain of interest. The (b) Canadian Earth System Model (CanESM2) grid at 2.81° horizontal resolution and (c) Global Precipitation Climatology Project (GPCP) grid at 1° horizontal resolution is also shown. The red horizontal line represents the equator.

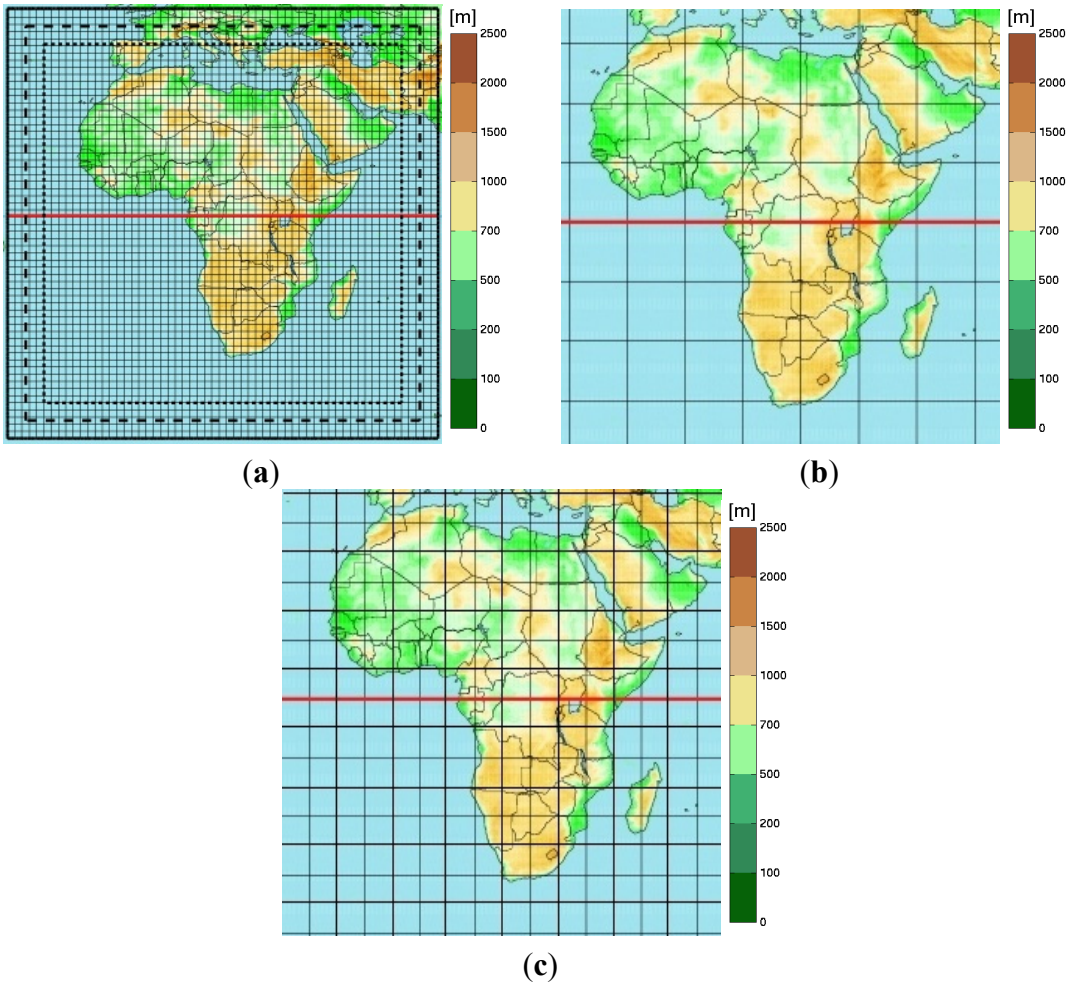

It should be noted though that the GPCP dataset may not be accurate for certain regions. For example, Nikulin *et al.* [52], based on a detailed analysis of the number of gauge stations included in the GPCC product, and therefore in GPCP, found that almost no station observations over central Africa (Angola, Democratic Republic of the Congo, Tanzania and Mozambique) were used for any of the months for the 1998–2006 period. This may have influenced the quality of the dataset over this region.

2.3. Methods

The objective of this article is two-fold. The first objective is to assess performance and boundary forcing errors (discussed below) associated with CRCM5 simulated dry spell characteristics and the added value of CRCM5 over the driving GCM, *i.e.*, CanESM2. The second objective is to assess projected changes to dry spell characteristics from CRCM5 transient climate change simulations for the RCP 4.5 scenario. It must be noted that all analysis presented in this article are performed on

respective grids. In other words, CanESM2 and GPCP data were not interpolated to CRCM5 grid, unless otherwise specified.

The dry spell characteristics considered in this study include the mean annual and seasonal number of dry days, dry spells and five-year return levels of annual and seasonal maximum dry spell duration, defined as the statistical estimate of the annual and seasonal maximum dry spell duration that would occur on average once every five years. The seasons considered correspond to the boreal (July–September; JAS) and austral (January–March; JFM) summers. In the present study, a dry day is defined as a day with a precipitation amount less than a predefined threshold. This threshold is subjective and, in this study, 0.5 mm, 1 mm, 2 mm and 3 mm are considered. As in previous studies [53–55] dry spell is defined as an extended period of dry days, including those of one day duration.

The return levels of dry spell durations are computed using the peaks-over-threshold (POT) approach. The advantage of the POT over the annual/seasonal maximum approach is that it considers those extreme values that are larger than some of the annual/seasonal maximum extremes that will not normally be considered in the annual/seasonal maximum approach [10,55]. In this approach, the average number of dry spell durations per year/season (say λ) are set a priori and the largest $n\lambda$ values are selected, from the n years considered. In this study, λ varies from 1 to 2 depending on the region. For the tropics where the number of dry spells is large, λ is set to 2, while for the subtropics, λ varies from 1 to 2 and for the Sahara λ is set to 1 since the number of dry spells are small though they are of very long durations. This approach strategy is equivalent to fixing the threshold at the, say, 95th or 98th percentile value [56]. For probabilistic modelling of POT values, the General Pareto Distribution (GPD) is used [10].

2.3.1. Performance Errors

The performance errors are assessed by comparing dry spell characteristics, *i.e.*, number of dry days, number of dry spells and return levels of maximum dry spell durations derived from the ERA-Interim driven CRCM5 simulation, for the current 1997–2008 climate, with those derived from GPCP [51] analysis. The 1997–2008 period was chosen since GPCP is only available for this period. The performance errors are assessed for various characteristics at annual and seasonal time scales, except for the number of dry spells where, the total number of dry spells for the 12-year period is considered; this is to include the dry spells that will extend from the end of a given year to the beginning of the next year. For the computation of return levels, since the comparison period is the 12-year period, with λ for the POT analysis varying from 1 to 2, 12 to 24 maximum dry spell durations are considered. The five-year return levels of maximum duration of dry spell are computed for all land points, and are masked in grey at those grid points where the return levels of maximum duration of dry spells are found larger than 365 (93) days in the case of annual (seasonal) maximum dry spells. The five-year return period is chosen since the number of years for which observation data is available is only 12 years. Return levels corresponding to higher return periods will have larger uncertainties given the small sample size and are therefore not considered. Though analysis has been performed for all four thresholds, validation results will be presented only for 0.5 mm and 3 mm threshold for the dry

spell characteristics. Where appropriate, results for other thresholds, *i.e.*, 1 mm and 2 mm are discussed.

2.3.2. Boundary Forcing Errors

In addition to performance errors, the CRCM5_CanESM2 simulations will have additional errors due to errors in the nesting CanESM2 data since RCMs are strongly influenced by the large-scale circulation from driving GCMs [57]. These errors, referred to as boundary forcing errors, are assessed by comparing CRCM5 driven by CanESM2 with CRCM5 driven by ERA-Interim. Reducing boundary forcing errors requires that the GCM provides more realistic boundary values.

2.3.3. Added Value

The added value of the RCM is the ability to improve the representation of the regional to local climate compared to the more coarsely resolved global climate models. In other words, RCM can provide additional detail for regions with important orography, land-sea contrasts and changes in surface type. The small-scale atmospheric features such as convective cells that are not well represented in the global climate models are better captured in RCMs. The added value is assessed by comparing the CRCM5_CanESM2 simulation with CanESM2 simulation.

2.3.4. Projected Changes

The projected changes to dry spell characteristics for two future time slice windows, *i.e.*, 2041–2070 and 2071–2100 are assessed by comparing the future dry spell characteristics with those for the current 1981–2010 period of the CRCM5_CanESM2 simulation. All figures corresponding to projected changes show absolute changes, *i.e.*, $X_f - X_c$, where X_f and X_c are the future and current values of the variable of interest X. However, reference in terms of percentage changes is also used where required, which is computed as $\left(X_f - X_c\right) / X_c$. Projected changes are also assessed based on CanESM2 simulation for the same two future periods. For the computation of return levels, using POT, for the current and future 30-year time slices, the values of maximum dry spell durations considered can vary from 30 up to 60. Projected changes for grid points where the return levels of maximum duration of dry spells are found larger than 365 (93) days in the case of annual (seasonal) maximum dry spells for current and/or future climates are masked in grey color. The results related to projected changes are presented only for the 2 mm threshold and other thresholds are discussed as required.

The statistical significance of projected changes to the mean number of dry days and dry spells is assessed using the Student's t-test [58] at 95% confidence level, while the nonparametric vector bootstrap resampling method [59–61] is used for return levels of maximum dry spell duration. The 95% confidence interval for return levels is calculated as: R0 ± 1.96SE, where R0 is the sample return level and SE is the standard error of the return level estimated using 1000 bootstrap resamples. Such confidence intervals for return levels are calculated for each grid-point for both future and current climates. The statistical significance of the difference between the future and current period values is

assessed using these confidence intervals, *i.e.*, the change (positive/negative) is considered significant if these confidence intervals do not overlap.

3. Results

3.1. Assessment of Errors and Added Value

3.1.1. Performance Errors

As discussed under the methods section, performance errors are assessed by comparing CRCM5_ERA_Interim and GPCP for the 1997–2008 period. Figure 2a shows the spatial distribution of annual mean number of dry days for the precipitation thresholds of 0.5 mm and 3 mm. GPCP shows minimum values of dry days in the tropics where strong convective precipitation occurs. The lowest values of annual number of dry days in the 120–240 days range is located in the Democratic Republic of Congo, along the South-East coast of Africa and in the mountainous regions of the eastern Madagascar, the East Africa Highlands and the elevated terrain of Ethiopia and Sudan. The maximum number of dry days are, as expected, in the subtropics where the deserts are located. For northern-most and southern-most parts of Africa, the values of dry days are generally regulated by the passage of mid-latitude fronts [1]. Annually, CRCM5_ERA_Interim overestimates the mean number of dry days in the tropics and in the sub-tropics compared to GPCP, while it underestimates along the eastern coast of Africa starting from South Africa and extending to the south of Somalia. As the precipitation threshold increases, the number of dry days increases. For example, in the Central African Republic, the number of dry days in the 180–210 range for 0.5 mm increases to the 210–240 range for the 3 mm threshold. The spatial patterns are more similar at the 2 mm and 3 mm threshold for GPCP and CRCM5_ERA_Interim.

The seasonal number of dry days in the tropics changes with the migration of the Inter Tropical Convergence Zone (ITCZ) from its northern most position in boreal summer to its southern position during the austral summer. Figure 2b shows that in the boreal summer, GPCP shows a minimum number of dry days to the north of the equator, where it precipitates the most, due to the northerly position of ITCZ during this season. In the sub-tropics, *i.e.*, the regions of Sahara and Kalahari deserts, the values of dry days are found larger. As the threshold is increased from 0.5 mm to 3 mm, the number of dry days increases especially in the ITCZ region; dry days in the 10–25 range at 0.5 mm increase to the 25–40 range at a 3 mm threshold. In the austral summer (Figure 2c), GPCP shows minimum values in the ITCZ region, *i.e.*, south of the Equator during this season, and higher values are located in the Sahara desert. For boreal summer, CRCM5_ERA_Interim overestimates the number of dry days in the Sahel (Mali, Niger, Chad) compared to GPCP. This is due to the southward bias in the position of the Sahara Heat Low that does not move enough north, which results in a narrower West African Monsoon rainfall band [30]. For both austral and boreal summers (Figure 2b,c), CRCM5_ERA_Interim generally underestimates the number of dry days especially in the tropics compared to GPCP. However, it was shown in a previous CRCM5 study [30] that for some regions such as the Gabon, Democratic Republic of Congo and Madagascar, CRCM5 driven by ERA-Interim simulates more realistic precipitation than GPCP. In these regions, GPCP misses the rainfall peak.

Figure 2. Number of dry days at 0.5 mm (top) and 3 mm (bottom) thresholds for the (**a**) annual, (**b**) boreal summer (JAS) and (**c**) austral summer (JFM) for CRCM5 driven by ERA-Interim (middle left) and CanESM2 (middle right), CanESM2 (extreme right) and GPCP (extreme left), for the 1997–2008 period.

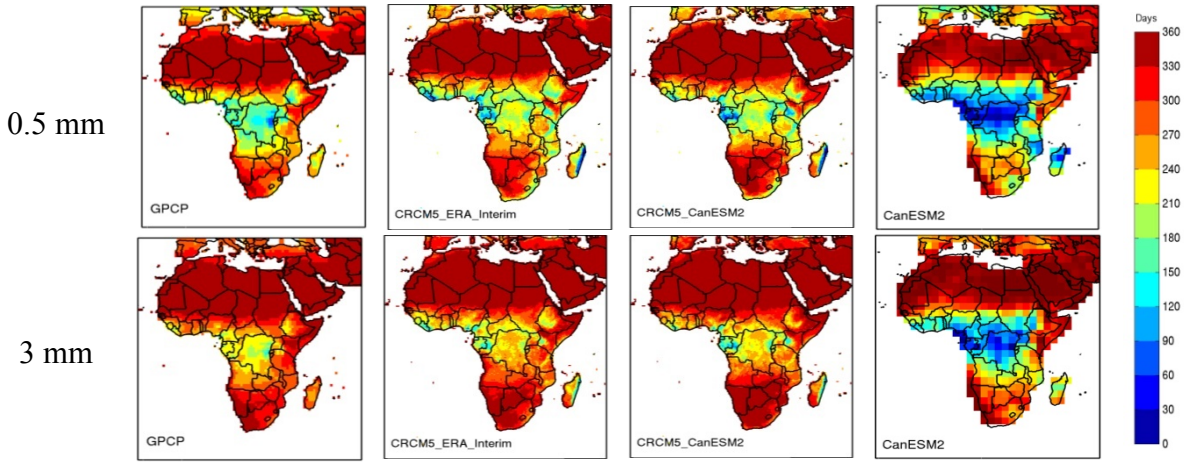

(**a**) Annual

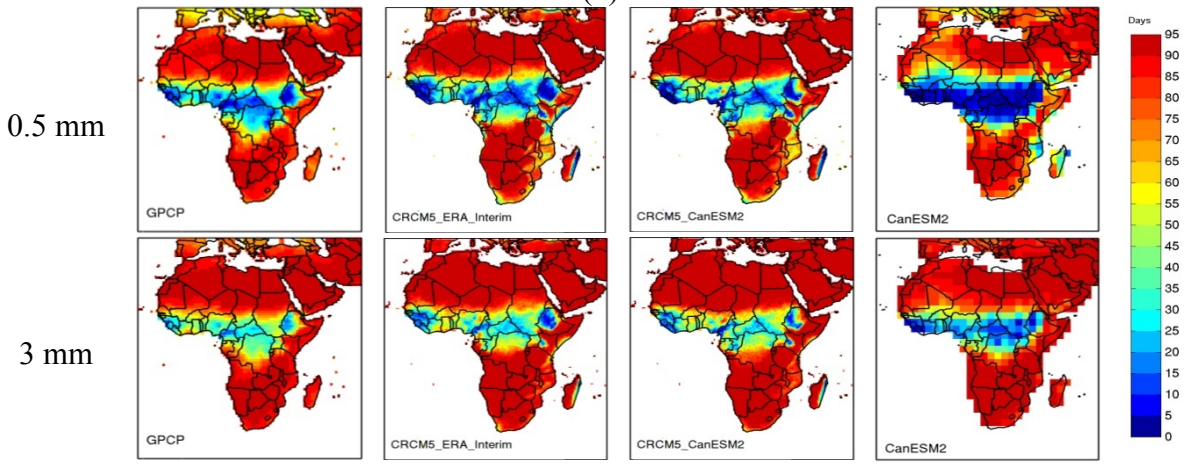

(**b**) Boreal summer (JAS)

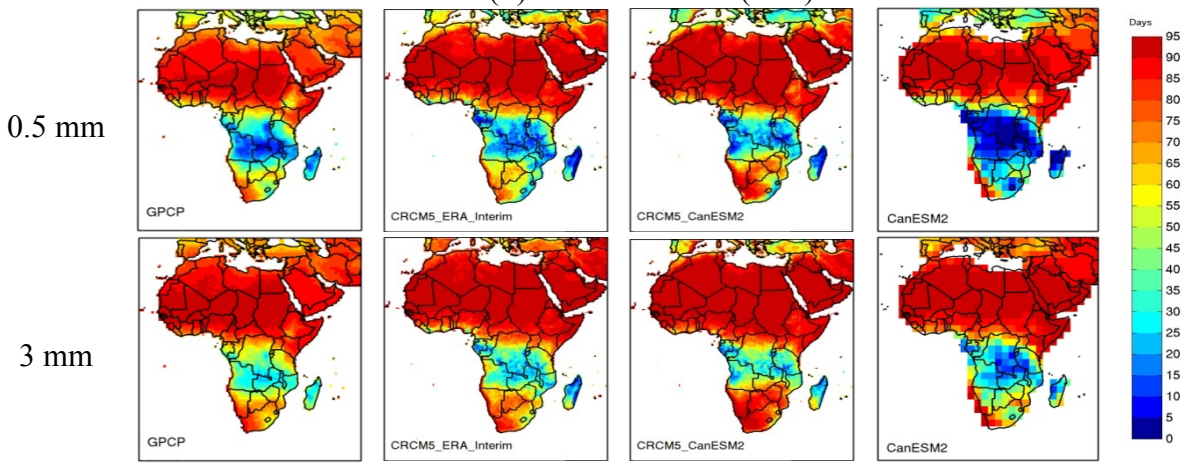

(**c**) Austral summer (JFM)

Figure 3. Number of dry spells at 0.5 mm (top) and 3 mm (bottom) thresholds for the (**a**) total 12 years, (**b**) boreal summer and (**c**) austral summer period for CRCM5 driven by ERA-Interim (middle left), and CanESM2 (middle right), CanESM2 (extreme right) and GPCP (extreme left), for the 1997–2008 period.

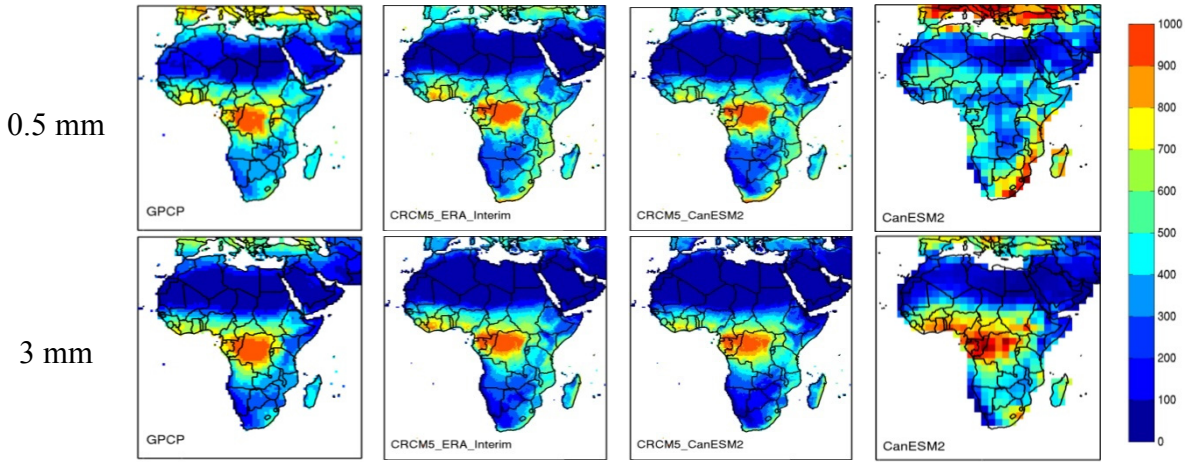

(**a**) 12 years

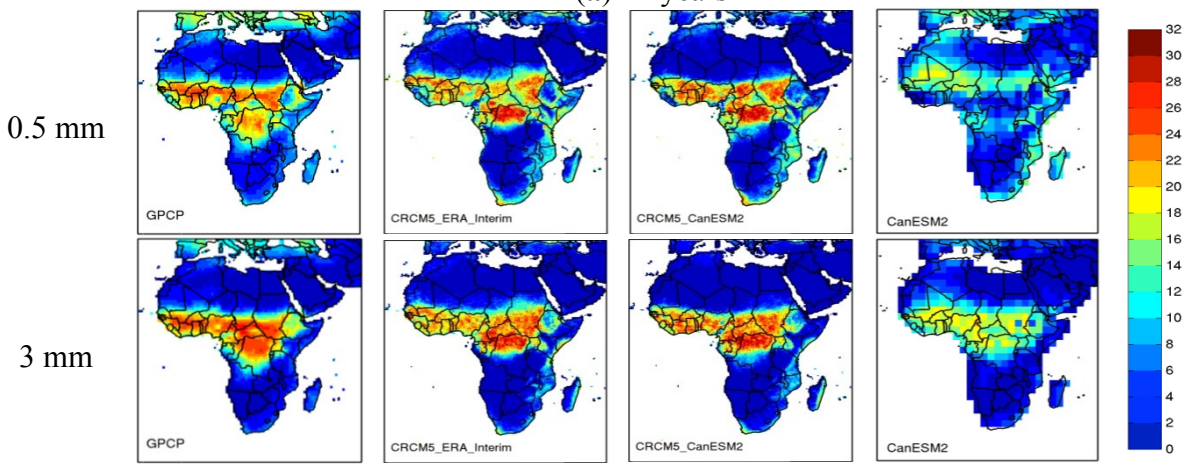

(**b**) Boreal summer (JAS)

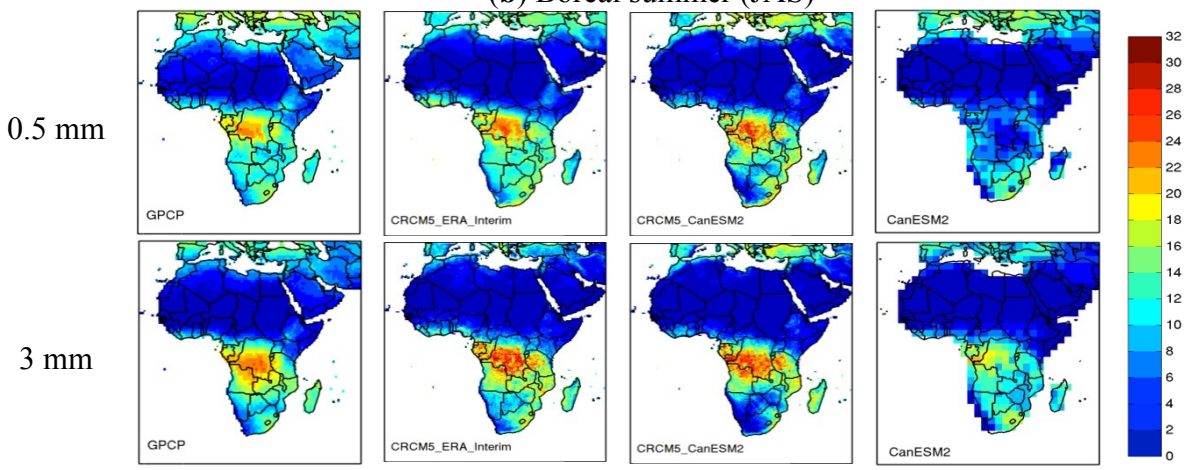

(**c**) Austral summer (JFM)

The total number of dry spells at 0.5 mm and 3 mm thresholds for CRCM5_ERA_Interim are now compared with GPCP (Figure 3a) for the 1997–2008 period. GPCP shows high values of number of dry spells in the tropics where there are many days with precipitation, which leads to several short dry

spells. GPCP shows in the subtropics small number of dry spells because of the small number of precipitation days that leads to longer dry spells. High values of the number of dry spells are also seen along the northern coast of the Maghreb (Morocco-Algeria-Tunisia) and the southeast coast of South Africa, particularly at 0.5 mm. Figure 3a shows that CRCM5_ERA_Interim underestimates the values in the Kalahari desert and in the tropics but overestimates the number of dry spells along the eastern coast of Africa extending from the South of Somalia to the South of Africa and also the Guinean coast of Africa compared to GPCP. In fact, for the south coast of South Africa, CRCM5_ERA_Interim shows number of dry spells in the 700–800 range, while GPCP has dry spells in the 400–500 range at 0.5 mm threshold. These results are consistent with the underestimation of the mean number of dry days (Figure 2) linked with the model tendency to precipitate more, for instance, frequent change between wet and dry spells in the model simulation. As the threshold increases, the mean number of dry spells decreases.

For the boreal summer (Figure 3b), the observed (*i.e.*, GPCP based) maximum number of dry spells are collocated with the position of the ITCZ at around 10°N latitude, while in the austral summer (Figure 3c), the observed maximum of number of dry spells shift with the position of the ITCZ to around 10°S latitude. For the boreal summer, CRCM5_ERA_Interim represents the narrow rain belt in the tropics reasonably well. At 0.5 mm and 3 mm thresholds, CRCM5_ERA_Interim overestimates the mean number of dry spells along the eastern coast of Africa extending from South of Somalia to South Africa. In the tropics, CRCM5_ERA_Interim generally overestimates the mean number of dry spells. Annually and seasonally, CRCM5_ERA_Interim agrees better with GPCP with maximum values located in the Democratic Republic of Congo and lower values in the desert regions (Sahara and Kalahari).

As mentioned earlier, the return levels of maximum annual/seasonal dry spell duration are computed using the POT approach**,** with λ varying from 1 to 2 (Figure 4). Grey colors are used for grid cells where the annual (seasonal) maximum dry spell duration is higher than 365 (93) days. It should be noted that the points that are masked vary for GPCP and model simulations. The GPCP based five-year return levels of annual maximum dry spell durations have low values in the tropics (where it rains the most), which is consistent with the large number of dry spells of shorter duration for that region. High return values are found in the southern part of Africa in the vicinity of the Kalahari Desert (Angola, Botswana). Eastern Madagascar, East Africa Highlands and the elevated terrains of Ethiopia and Sudan also have low values of dry spell duration since it rains more frequently.

For the five-year return levels of annual maximum dry spell duration (Figure 4a), GPCP shows that the values are in the range of 40 consecutive days in the tropical region, while in the subtropics, the values are larger. In general, CRCM5_ERA_Interim overestimates the annual maximum dry spell duration compared to GPCP. The differences are larger in both Sahara and Kalahari deserts where CRCM5_ERA_Interim has too many consecutive dry days. For boreal summer (Figure 4b), CRCM5_ERA_Interim overestimates the five-year return level especially in the north of the Democratic Republic of Congo. In fact, CRCM5_ERA_Interim shows values in the 50–70 range, while GPCP values are less than 30 at the 3 mm threshold. CRCM5_ERA_Interim also overestimates return levels in the Mediterranean region.

In austral summer (Figure 4c), CRCM5_ERA_Interim overestimates the return levels in the Sahara desert and in the Sahel compared to GPCP. As the threshold increases from 0.5 to 3 mm, the maximum

dry spell duration increases. The annual and boreal summer figures for the Guinean coast (near Gabon and Liberia) shows that the difference between the 3 mm and 0.5 mm threshold is very small which means that the daily precipitation rate is often higher than 3 mm threshold.

Figure 4. Same as Figure 2, but for the five-year return levels of the maximum dry spell duration. The grid points are masked in grey color where the return levels are larger than 365 days in the case of (**a**), and 93 days for the cases of (**b**) and (**c**).

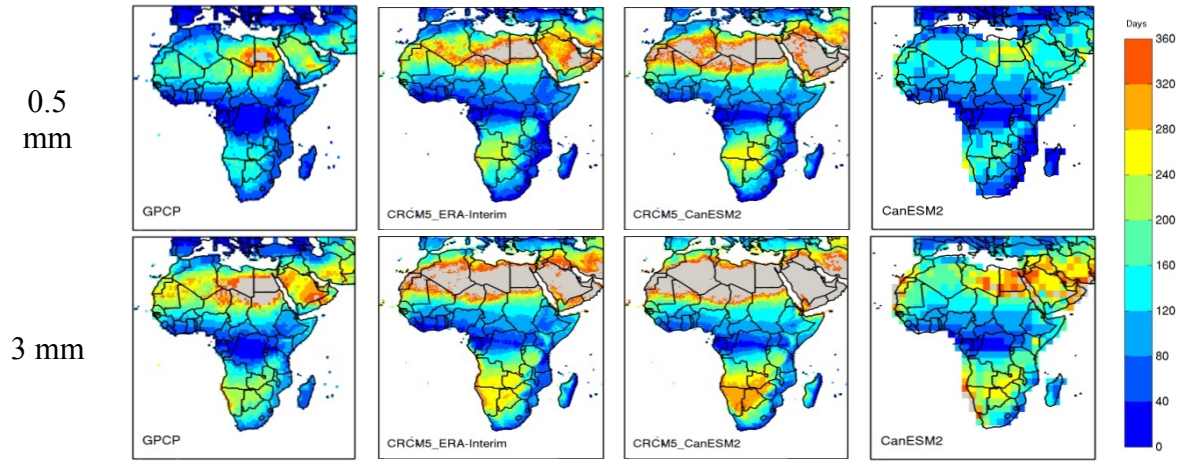

(**a**) Annual

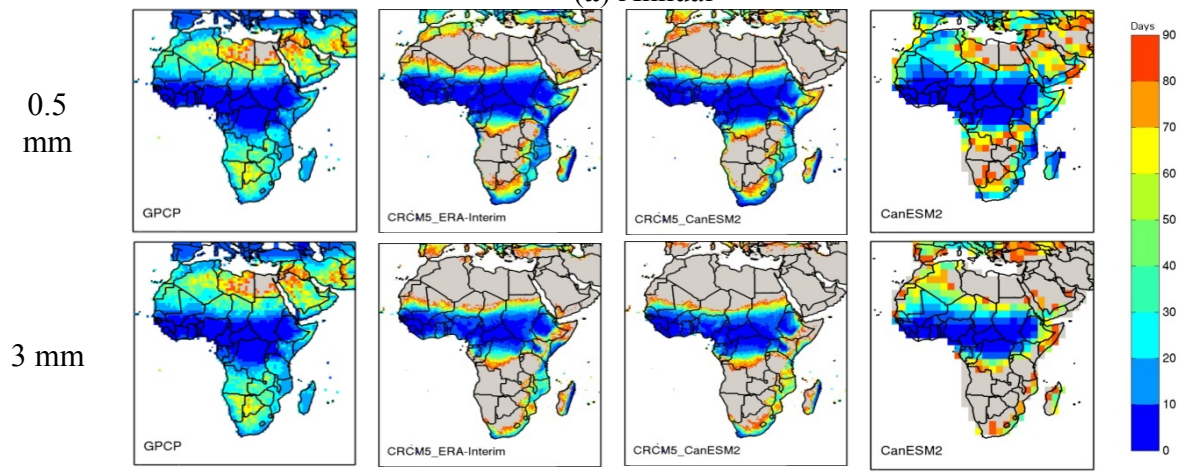

(**b**) Boreal summer (JAS)

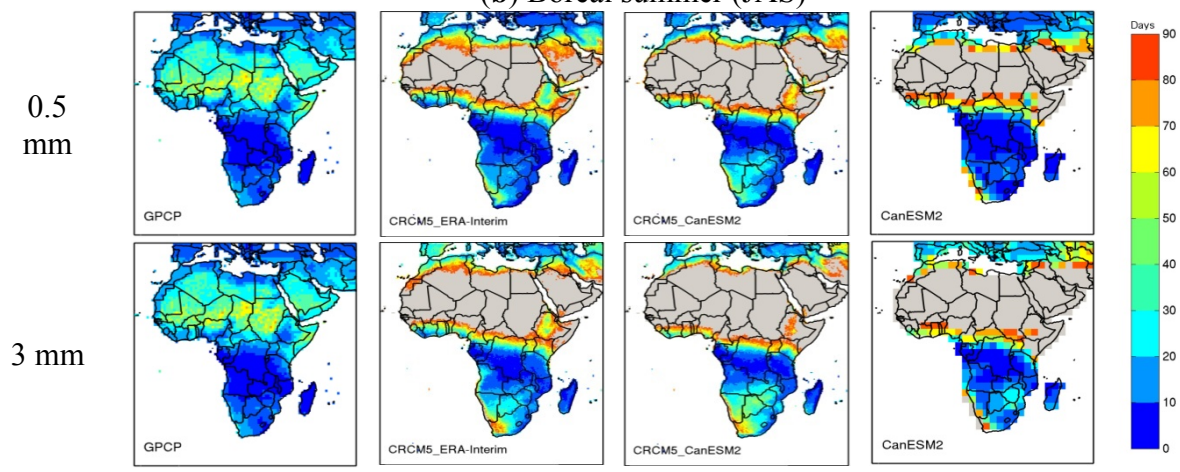

(**c**) Austral summer (JFM)

3.1.2. Boundary Forcing Errors

As discussed previously, boundary-forcing errors are assessed by comparing CRCM5_CanESM2 and CRCM5_ERA_Interim simulations. Since precipitation will have a direct influence on the dry spell characteristics, precipitation in CRCM5_ERA_Interim and CRCM5_CanESM2 are first compared. Figure 5 shows that the boreal summer (annual) precipitation is larger (smaller) for CRCM5_CanESM2 compared to CRCM5_ERA_Interim for the Guinean coast, but there are a number of other differences in the two experiments. The CRCM5_CanESM2 is wetter over the north-eastern southern Africa in the annual mean. It is also wetter over sub-tropical southern Africa especially in austral summer. On the other hand, the CRCM5_CanESM2 is dryer over north-western equatorial/tropical Africa (notably in Liberia and Sierra Leone) and in Ethiopia, especially in the boreal summer. It was also shown in a previous study [31] that CRCM5_CanESM2 has difficulties in representing the precipitation over the West African Monsoon region, and that only CRCM5_ERA_Interim was able to reproduce the seasonal migration of the West African Monsoon precipitation. The inability of CRCM5_CanESM2 to well simulate the rainy season in the West African Monsoon is related to the misrepresentation of the seasonal cycle of the GCM-simulated SSTs in the equatorial Atlantic Ocean [31].

Figure 5. Annual (top row), boreal (middle row) and austral (bottom row) summer mean (1997–2008) precipitation for GPCP (extreme left), CRCM5 driven by ERA-Interim (middle left), CRCM5 driven by CanESM2 (middle right) and CanESM2 (extreme right), for the 1997–2008 period.

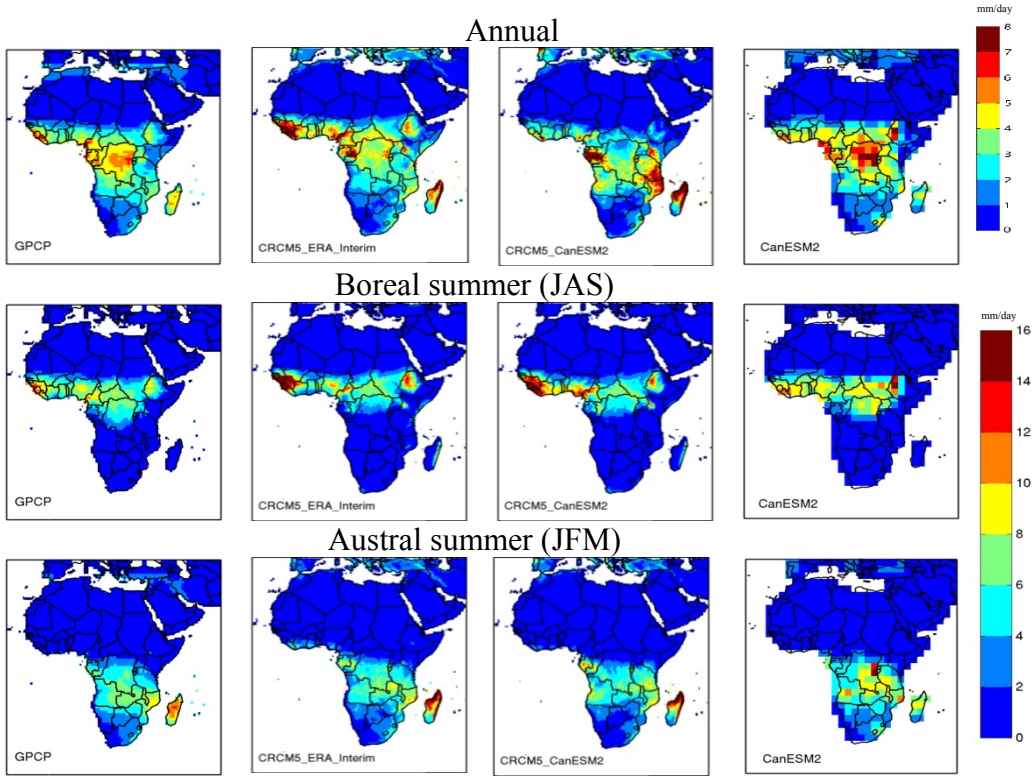

The difference between CRCM5_CanESM2 and CRCM5_ERA_Interim simulated dry spell characteristics show that, in general, CRCM5_CanESM2 has positive boundary forcing errors, *i.e.*,

more number of dry days, along the Guinean coast for the annual mean (Figure 2a), while for the same region, negative boundary forcing errors are noted for the boreal summer (Figure 2b). CRCM5_CanESM2 has positive boundary forcing errors over the north-eastern southern Africa, while negative errors are noted over the north-western equatorial region in austral summer (Figure 2c). For the number of dry spells, CRCM5_CanESM2 exhibits negative boundary forcing errors, *i.e.*, less number of dry spells in the Guinean coast for the annual mean (Figure 3a), while for the same region, CRCM5_CanESM2 shows positive errors for boreal summer (Figure 3b). In austral summer (Figure 3c), positive boundary forcing errors over the north-western equatorial region can be seen. For the five-year return levels associated with annual and austral summer maximum dry spell duration (Figure 4a,c), CRCM5_CanESM2 has a positive boundary forcing errors in south central Africa and in the Ethiopian highlands compared to CRCM5_ERA_Interim while in boreal summer (Figure 4b), positive boundary forcing errors are found for the Horn of Africa and Maghreb regions.

Comparing the lateral boundary forcing errors of the three dry spell characteristics considered here, those associated with the return levels of maximum dry spell duration are larger than those for the mean number of dry days and mean number of dry spells, especially over south central Africa. Comparison of performance errors and lateral boundary errors show that, in general, performance errors associated with the annual and seasonal dry spell characteristics are larger in magnitude compared to the lateral boundary forcing errors, particularly for austral summer.

3.1.3 Added Value

For many regions over Africa, CRCM5_CanESM2 improves representation of the dry spell characteristics compared to CanESM2. As an example, for the mean annual number of dry days (Figure 2a), CRCM5_CanESM2 (third column) has more dry days in the tropics compared to CanESM2 (fourth column), and therefore, is in better agreement with GPCP (first column). The CanESM2 daily precipitation rate is relatively high compared to GPCP and CRCM5. The same is observed for the boreal and austral summers.

CRCM5_CanESM2 also represents better the number of dry days and the number of dry spells (Figures 2 and 3) compared to CanESM2. Thus, CRCM5_CanESM2 exhibit clear added value compared to CanESM2 for the dry days and the number of dry spells. The added value is less obvious though in the case of return levels (Figure 4).

3.2. Projected Changes to Dry Spell Characteristics

In this section, projected changes to dry spell characteristics over Africa for RCP 4.5 scenario are evaluated as differences between the future 2041–2070 and 2071–2100 periods and the current 1981–2010 period of the CRCM5_CanESM2 simulation. Projected changes are also assessed based on CanESM2 simulation. It should be noted that the projected changes are presented as absolute differences. However, reference in terms of percentage changes are used where appropriate. Here, the results of projected changes are presented for the 2 mm threshold. Where relevant, results for other thresholds are discussed.

Figure 6 shows projected changes to the mean annual number of dry days as simulated by CRCM5_CanESM2 and CanESM2 at 2 mm threshold. CRCM5_CanESM2 and CanESM2 show some significant increases, according to the t-test at 95% confidence level for the tropics, with the absolute changes increasing from 2041–2070 to 2071–2100. For CRCM5_CanESM2, in relative terms, the number of dry days increases by 0–30% (0–45%) for the future 2041–2070 (2071–2100) period. The spatial extent of the region with significant increase in the tropics is much larger for CanESM2 compared to CRCM5_CanESM2. For the Horn of Africa, CanESM2 shows scattered significant decreases for the 2041–2070 period, which is also visible for the 2071–2100 period; no significant changes are noted for the region in CRCM5_CanESM2. Conflicting climate change signal can be noticed for more regions. As an example, in some parts of the Maghreb (Tunisia, Algeria, Morocco, Libya), CRCM5_CanESM2 shows a significant increase, while CanESM2 shows a significant decrease for the 2071–2100 period.

Figure 6. Annual mean number of dry days as simulated by CRCM5 driven by CanESM2 (**a**–**c**) and CanESM2 (**d**–**f**) for the present (1981–2010) (a,d) and the corresponding projected changes for the 2041–2070 (b,e) and the 2071–2100 (c,f) periods for RCP 4.5 scenario for 2 mm threshold. Grid cells where projected changes are not statistically significant at 95% confidence level are shown in white.

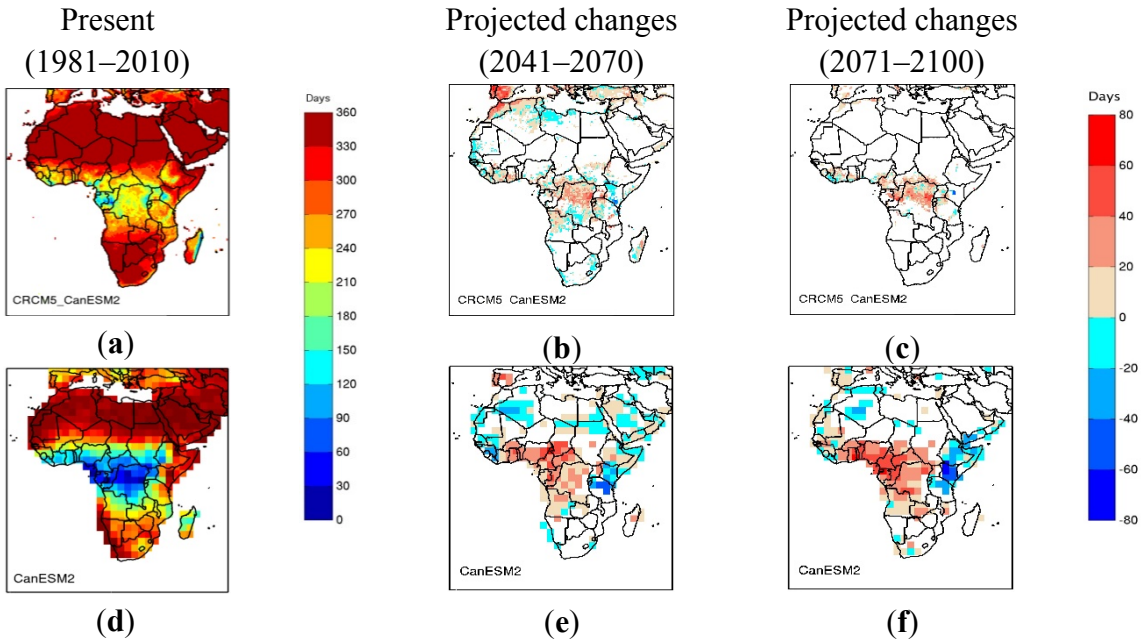

Significant increase in the mean number of dry days for the boreal summer (Figure 7) is noted for some regions of the tropics for CRCM5_CanESM2, especially in the western parts of the tropics where the increase is around 60% (16–24 range in terms of absolute change) by the end of the 21st century. Significant increases in dry days for the tropics are also shown by CanESM2 and the magnitude of changes increases from the 2041–2070 period to the 2071–2100 period. CRCM5_CanESM2 shows significant decrease in dry days in the Sahel and in the eastern part of South Africa. Though not significant, CRCM5_CanESM2 suggests some increases in the mean number of dry days in the Sahara and Kalahari deserts, while CanESM2 shows a decrease in the number of dry days where the Heat Low (near Algeria) is located.

Figure 7. Same as Figure 6, but for the mean number of dry days for boreal summer.

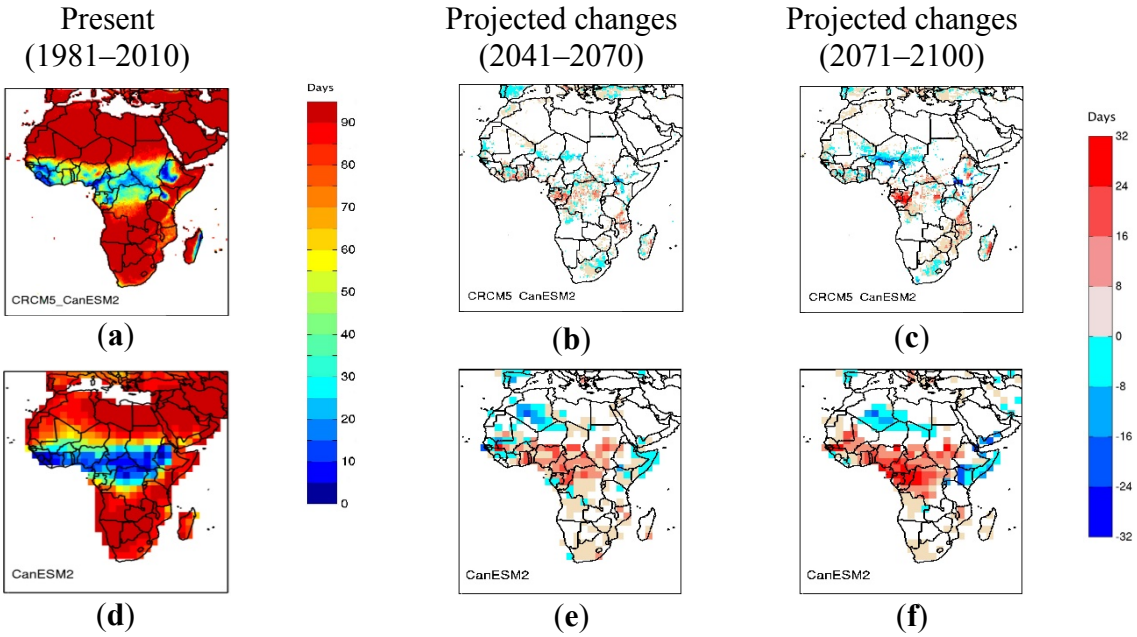

For austral summer (Figure 8), CRCM5_CanESM2 shows a significant increase in the mean number of dry days in the central tropics while some decrease is projected for the Horn of Africa, particularly for the 2071–2100 period. CanESM2 shows a significant increase in the central tropics for the 2041–2070 period followed by a significant decrease for the 2071–2100 period. For the western tropics region, CanESM2 shows a decrease in the dry days while CRCM5_CanESM2 shows an increase for the 2071–2100 period. Analysis of the soil moisture and precipitation fields for this region (figure not shown) indicate that, though precipitation and soil moisture are larger in CanESM2 compared to CRCM5_CanESM2, CanESM2 shows an increasing tendency in precipitation and soil moisture for the 2071–2100 period, while CRCM5_CanESM2 shows a clear decrease in precipitation and a non-significant decrease in soil moisture. The above appear to be responsible for the conflicting climate change signal in CRCM5_CanESM2 and CanESM2. However, CanESM2 is in agreement with CRCM5_CanESM2 for the central eastern part of Africa where significant decreases are projected for the 2041–2070 and 2071–2100 period.

Figure 9 shows projected changes to annual mean number of dry spells as simulated by CRCM5_CanESM2 and CanESM2 at 2 mm threshold. CRCM5_CanESM2 projects significant decreases in the annual mean number of dry spells from current to future for parts of the tropics and for the Maghreb. This decrease is consistent with the increase in the number of dry days that can lead to longer dry spells. On the other hand, CanESM2 shows significant increases and decreases in the tropics and a decrease in the south part of Africa (Namibia, Angola, Botswana, Zimbabwe, Zambia, Mozambique, South Africa, Lesotho, Swaziland). For the Horn of Africa, CanESM2 shows general significant decreases in the mean number of dry spells for the 2041–2070 period, followed by mostly significant increases for the 2071–2100 period. This is less evident in CRCM5_CanESM2 simulation. However, CanESM2 projection of the mean annual number of dry spells agrees with CRCM5_CanESM2 projection for the regions of South Africa and Horn of Africa at 2 mm threshold.

The contradictory climate signal for the tropics for CanESM2 and CRCM5_CanESM2 over the tropical region can also be due to the fact that daily precipitation in CanESM2 is often higher than

2 mm/day and therefore do not represent adequately dry spell characteristics at lower precipitation thresholds. The annual precipitation intensity for the 1981–2010 period vary spatially between 4 and 10 mm/day for CanESM2 in the tropics (figure not shown). Some preliminary analysis at 5 mm precipitation threshold revealed that both CanESM2 and CRCM5_CanESM2 project decreases in the mean number of dry spells for the 2041–2070 and 2071–2100 period (figure not shown).

Figure 8. Same as Figure 6, but for the mean number of dry days for austral summer.

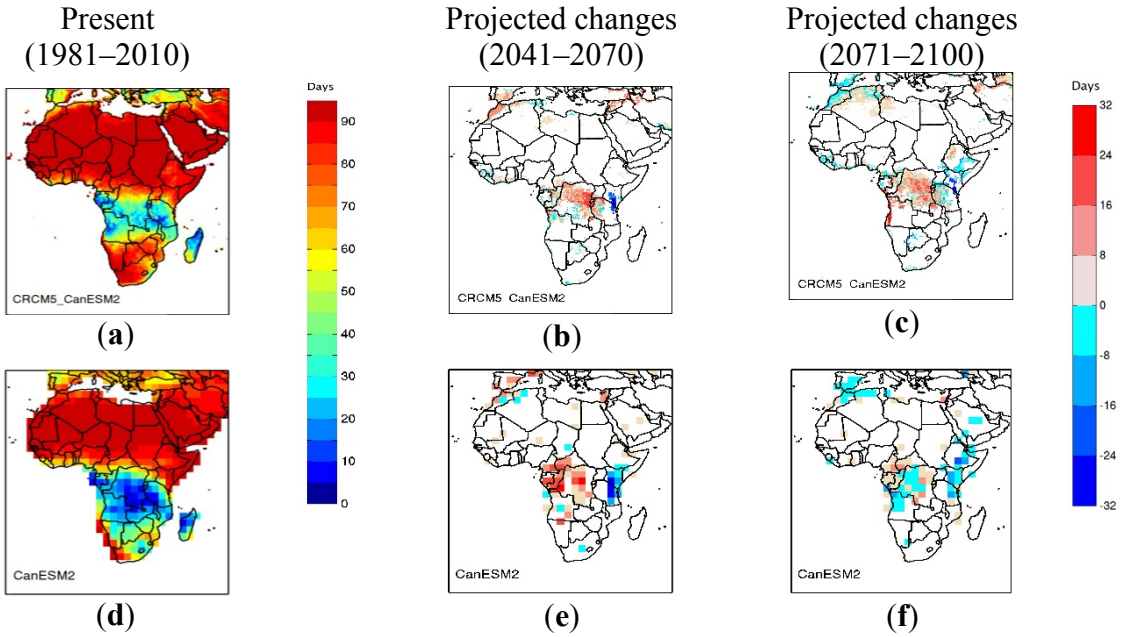

Figure 9. Same as Figure 6, but for annual mean number of dry spells.

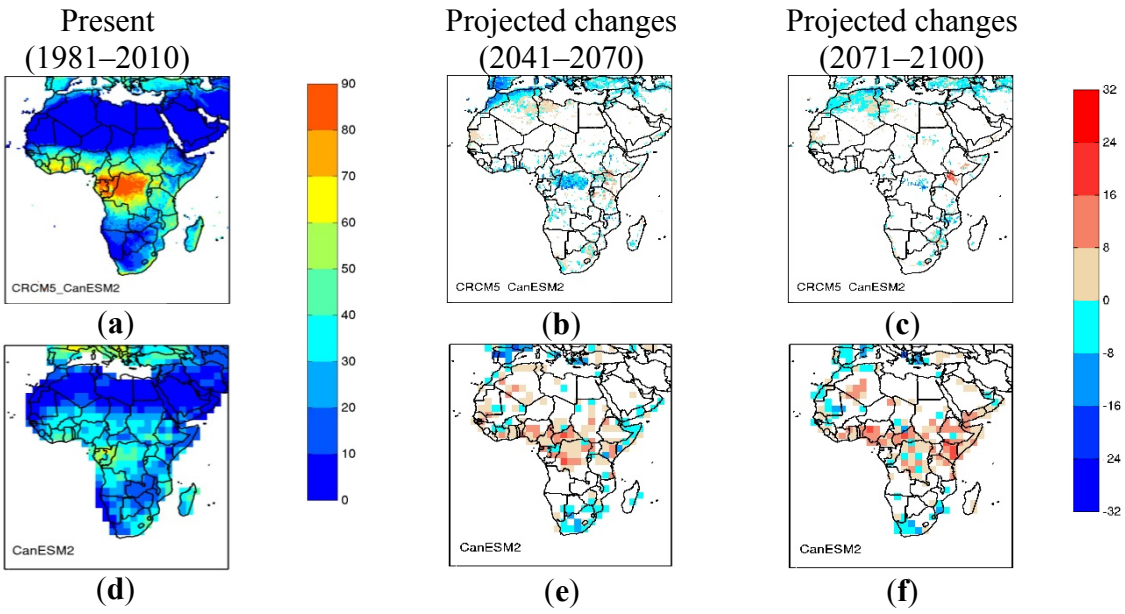

For the boreal summer (Figure 10), CRCM5_CanESM2 shows a decrease in the number of dry spells along the east coast starting from Somalia and extending to the South of Mozambique. The magnitude of the changes lies between −25% to −50% for the 2041–2070 period and between −50% to −75% for the 2071–2100 periods. However, CRCM5_CanESM2 and CanESM2 show important

differences for the tropics, the Sahel and the Maghreb regions. For the tropics, CRCM5_CanESM2 shows a general significant decrease with spotted increase while the CanESM2 shows mostly an increase. As discussed previously, CanESM2 has a higher daily precipitation rate and the choice of 5 mm and 10 mm thresholds (figure not shown) shows better agreement.

Figure 10. Same as Figure 6, but for the mean number of dry spells for boreal summer.

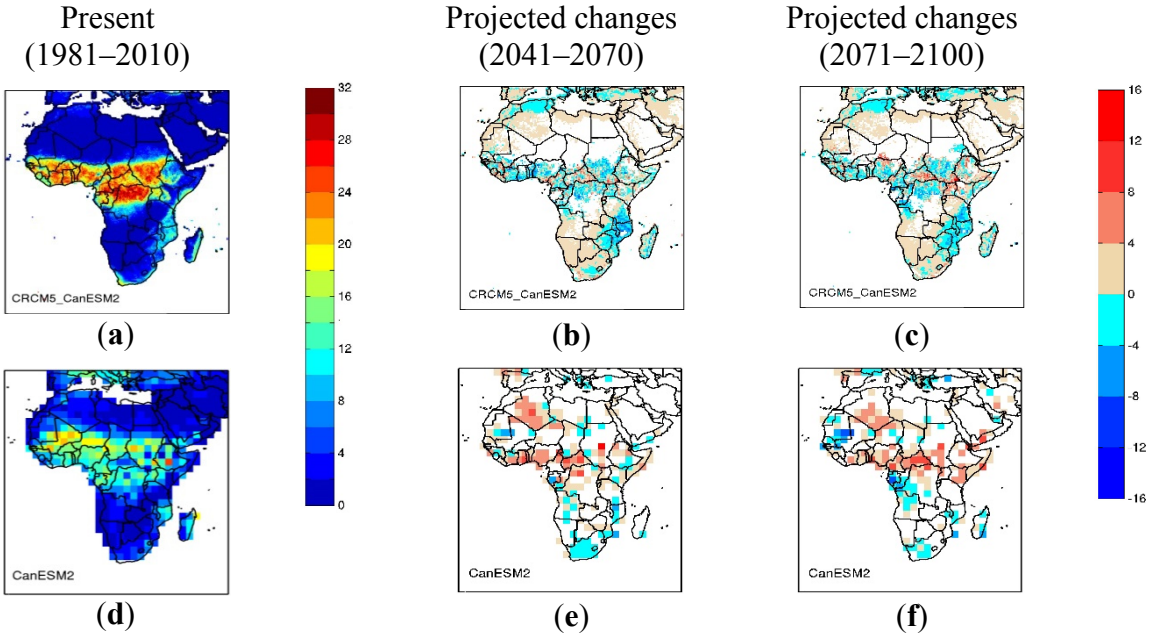

For the austral summer (Figure 11), CRCM5_CanESM2 shows a general significant decrease in the central part of Africa and in the Maghreb regions for the 2041–2070 and 2071–2100 period. A scattered significant increase in the mean number of dry spells can be noted in the Horn of Africa (Ethiopia, Somalia). For CanESM2, however, projected changes are in general not significant at 95% confidence level.

Figure 11. Same as Figure 6, but for the mean number of dry spells for austral summer.

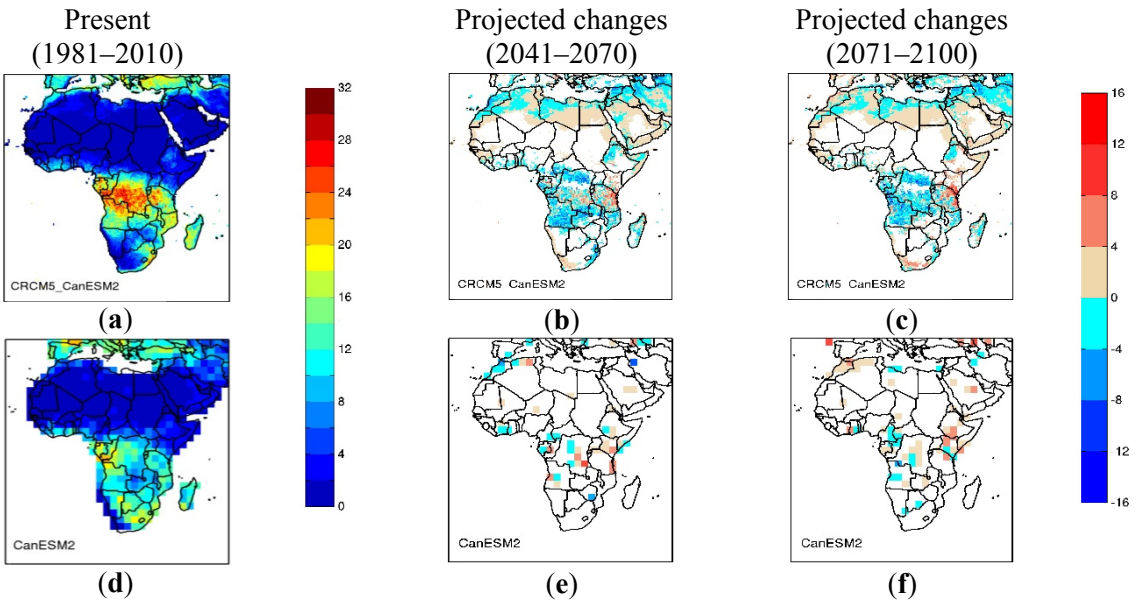

Figure 12 shows projected changes to the five-year return levels of the annual maximum dry spell duration at 2 mm threshold. The value of λ for a given grid-cell is constant in current and future climates. As discussed in the methodology, the return levels are computed using the GPD distribution. The statistical significance is assessed using the Bootstrap method at 95% confidence level. For CRCM5_CanESM2, the Sahara desert is masked (grey color in the figures) since most of the sampled maximum dry spell durations are equal to 365 days and therefore the calculation of the return levels cannot be performed satisfactorily. CRCM5_CanESM2 shows scattered significant increase in the tropics and along the east coast starting from Somalia and extending to the South of Mozambique. CRCM5_CanESM2 shows also significant increases in the northern part of the Maghreb, with absolute change in the 45–60 range for both periods. CanESM2 shows significant increases over a relatively large area in the tropics with absolute changes in the 15–30 range, for the 2041–2070 period, but is considerably reduced in extent for the 2071–2100 period.

Figure 12. Same as Figure 6, but for the 5-year return level of the annual maximum dry spell duration. The grid points where the return levels are larger than 365 days are masked in grey color.

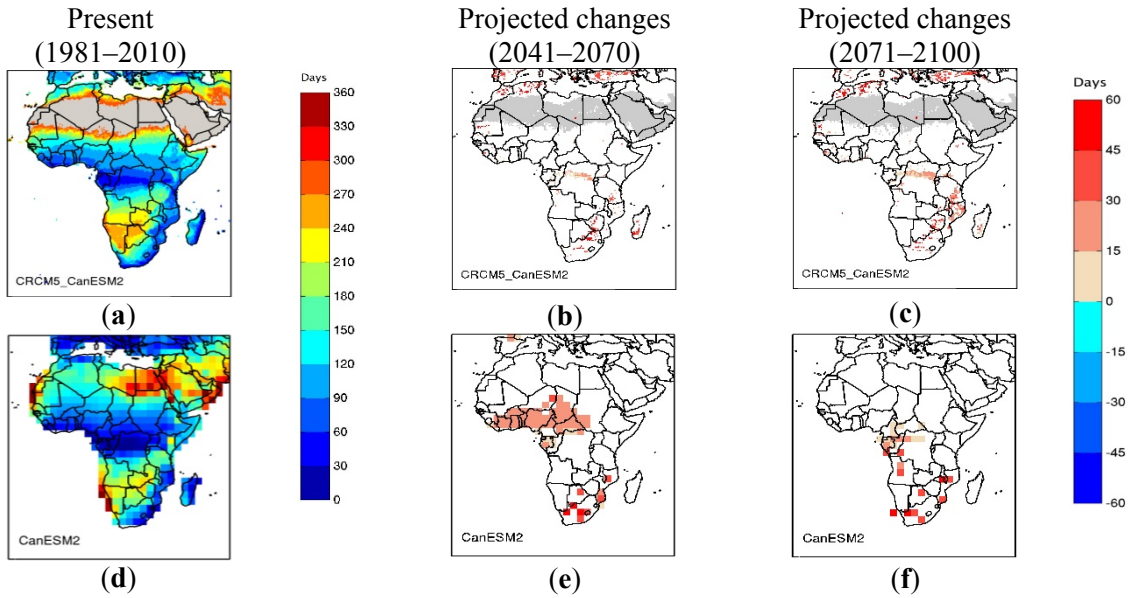

Figure 13 shows the 5-year return levels of the maximum dry spell duration for the boreal summer for the current period and their projected changes at 2 mm threshold. Notice here that both deserts (Sahara and Kalahari) are masked (grey color) for the same reason as mentioned previously. Here, calculation of return levels were not performed for some grid points along the Equator for CanESM2, for the boreal and austral summers since the daily precipitation rate is often greater than 2 mm/day which leads to insufficient number of values of maximum dry spell duration. Very few points show significant changes to 5-year return levels in boreal summer in future climate for CRCM5_CanESM2 and CanESM2. CRCM5_CanESM2 shows a scattered significant increase in the 5-year return levels of maximum dry spell duration in the tropics for the two future periods. CanESM2 shows significant increases to the south-west of the Sahel for the 2041–2070 period, with absolute changes in the 5 to 15 range.

Figure 13. Same as Figure 6, but for the 5-year return level of the boreal summer maximum dry spell duration. The grid points where the return levels are larger than 93 days or where return levels were not computed due to insufficient values of maximum dry spell duration are masked in grey color.

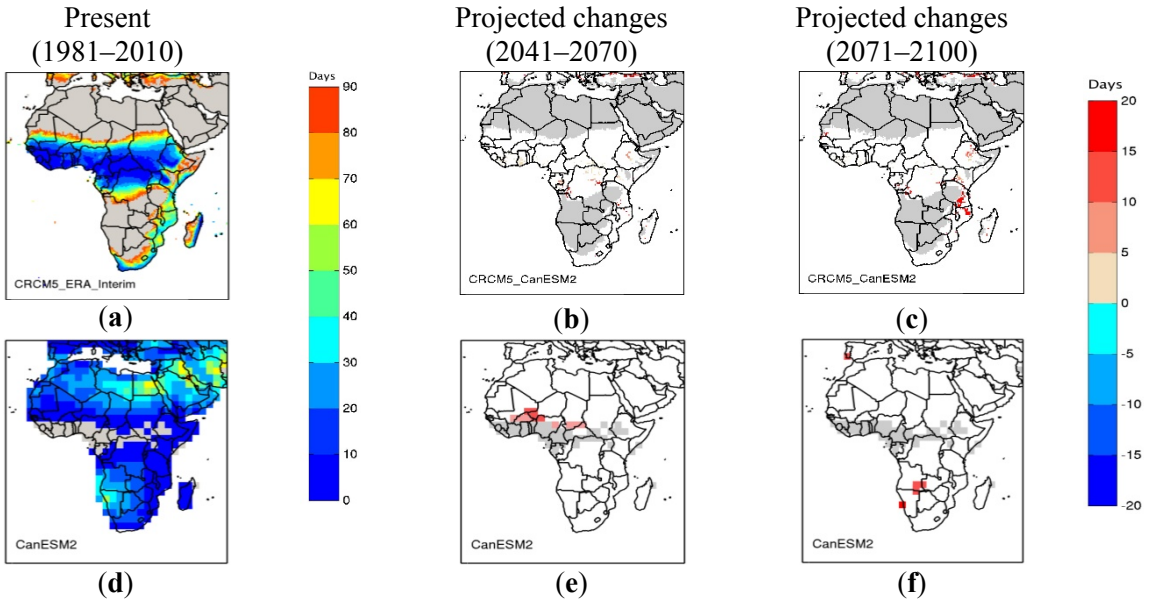

For the austral summer (Figure 14), significant increases in parts of the tropics are projected by CRCM5_CanESM2 for the future climate, with increasing magnitude from 2041–2070 to 2071–2100 period. An increase of the maximum dry spell duration is also seen in the north-eastern part of Maghreb region with a magnitude of 15 to 30% (15–20 range in terms of absolute change). No significant changes are noted for CanESM2. The results for 0.5 mm, 1 mm, and 3 mm thresholds are in general similar to those for 2 mm threshold.

Figure 14. Same as Figure 13, but for the austral summer.

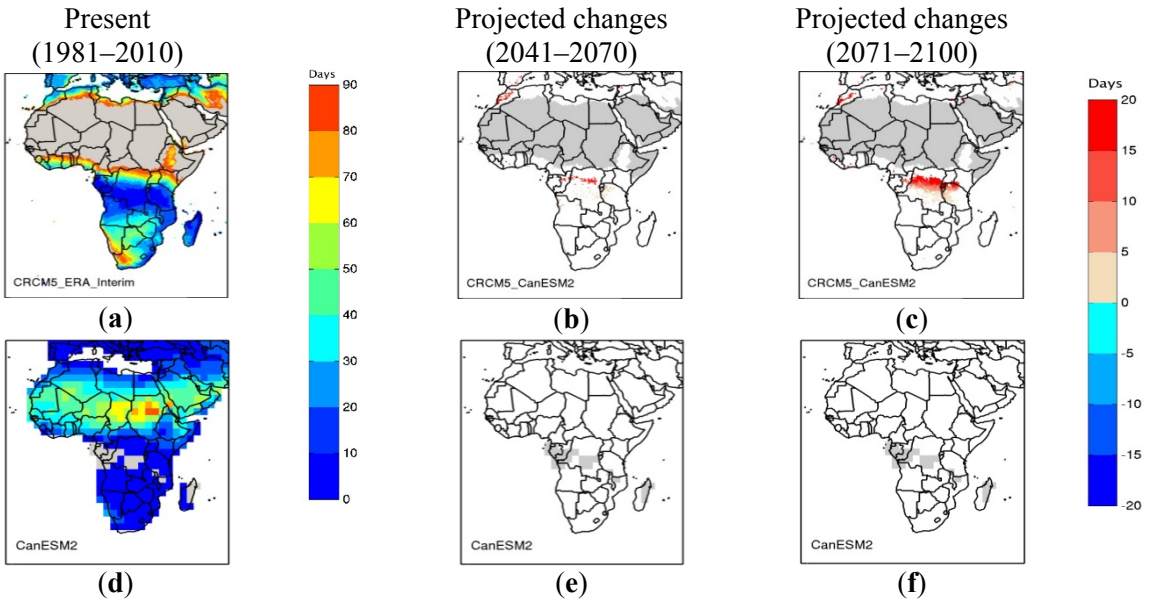

4. Discussion and Conclusions

In this study, we present an evaluation of errors—*i.e.*, performance and lateral boundary forcing errors—of selected dry spell characteristics over Africa as simulated by CRCM5 for different precipitation thresholds used to define a dry day. Also presented are the added value and projected changes to dry spell characteristics. The annual/seasonal dry spell characteristics considered are the mean number of dry days, mean number of dry spells and the five-year return level of the maximum dry spell duration. Performance errors are assessed by comparing the ERA-Interim driven simulation (CRCM5_ERA_Interim) with GPCP for the current 1997–2008 period. Boundary forcing errors are assessed by comparing the CanESM2 driven CRCM5 simulation (CRCM5_CanESM2) with CRCM5_ERA_Interim and finally added value of the RCM is assessed by comparing CRCM5_CanESM2 with CanESM2. The projected changes to dry spell characteristics for two future time slice windows, 2041–2070 and 2071–2100, corresponding to RCP 4.5 scenario, are then assessed by comparing the future characteristics with those for the current 1981–2010 period for both CRCM5_CanESM2 and CanESM2. A summary of the main results follows:

- The ability of CRCM5 in simulating dry spell characteristics in current climate is evaluated prior to the assessment of projected changes. The results for the various precipitation thresholds were similar (0.5 mm, 1 mm, 2 mm and 3 mm). Results suggest that the annual (seasonal) numbers of dry days are generally overestimated (underestimated) by CRCM5_ERA_Interim, *i.e.*, positive (negative) performance errors, particularly for North Equatorial Central Africa and Central Southern Africa regions, compared to GPCP. This overestimation in the annual mean number of dry days decreases with increasing precipitation thresholds. Consistent with these results, the annual (seasonal) number of dry spells are underestimated (overestimated) by CRCM5_ERA_Interim over the same regions. The five-year return levels of annual and seasonal maximum dry spell duration computed using the POT approach is generally overestimated by CRCM5_ERA_Interim.
- Results suggest that, in general, the performance errors are larger than the lateral boundary forcing errors. Performance errors can be reduced by further improving the representation of processes in the model such as convection, land-atmospheric interactions, West African Monsoon (WAM), while reduction of lateral boundary forcing errors require improved quality of the GCM data used as boundary conditions. CRCM5 reproduces the West African Monsoon, but fails to bring the precipitation far enough north into Sahel due to a weaker monsoonal flow associated with a cold bias in the Sahara as was also reported in Hernández-Díaz *et al.* [30]. This is the reason for the overestimation of dry days in that region. As for the tropics, it was noted that the soil moisture is generally underestimated in the model due to increased drainage in comparison with the Global Land Data Assimilation System (GLDAS) [62] database, which leads to less evaporation and therefore, a reduced number of precipitation days. Thus, better representation of land-surface processes is important as was pointed out by Taylor *et al.* [63] in their study over West Africa.
- The added value analysis showed that for many regions in Africa, CRCM5_CanESM2 improves local representation of the dry spell characteristics compared to CanESM2. In fact, CRCM5

driven by CanESM2 provides realistic spatial detail in the tropics since the regional model is able to capture the convection cells in the monsoon region more realistically, which is the main source of precipitation, due to its higher resolution compared to CanESM2.

- Analysis of the projected changes to dry spell characteristics revealed, that annually and seasonally in the tropics, CRCM5_CanESM2 shows significant increases in the number of dry days and in the five-year return levels of maximum dry spell durations. Analysis also showed significant decreases in the number of dry spells for the 2041–2070 and 2071–2100 periods. In other words, dry spells of longer durations can be expected in future climate with increasing magnitude from 2041–2070 to 2071–2100. For both periods, CanESM2 projections are similar to that of CRCM5_CanESM2 for the annual number of dry days and five-year return levels of annual maximum dry spell duration. However, conflicting climate change signal can be noted for the number of dry spells for the annual and boreal summer, where CRCM5_CanESM2 shows a significant increase while CanESM2 shows a significant decrease. This difference can partly be explained by the fact that CanESM2 is unable to reproduce the dry spell characteristics at lower precipitation thresholds.
- Projected changes to dry spell characteristics for the Horn of Africa are in general not found to be significant. However, CRCM5_CanESM2 shows some significant increase in the number of dry spells for boreal summer for the 2071–2100 periods. Similarly, for the Sahel region, projected changes to dry spell characteristics are not found significant, except for some significant decreases in the number of dry days for the boreal summer for the 2041–2070 and 2071–2100 periods for CRCM5_CanESM2.

Though the return levels presented in this study corresponds to the five-year return level period, many impact and adaptation studies would require information about higher return period. Analysis of projected changes to 10-, 20- and 30-year return levels (not shown) suggest increases for some parts of the tropics and in the south eastern part of Africa. The magnitude of absolute changes between the future period and the current climate increases with increasing return periods.

Changes in dry spell characteristics will have direct impact on climate sensitive sectors such as agriculture. More wet days combined with shorter dry spell duration during the growing season could be beneficial to the agriculture sector for regions such as the Horn of Africa and for some part of the Sahel for the 2071–2100 period. On the contrary, an increase in the number of dry days and in the maximum dry spell duration combined with less number of dry spells, but of longer duration, could affect agriculture adversely in the tropics and in the North of Africa.

In this study, the precipitation thresholds were selected subjectively following previous studies for other parts of the world. For practical applications, one would need to pick other thresholds. For example, for the tropics, evaporation is higher and therefore higher thresholds are desirable, as in Mupangwa *et al.* [64], where a 4.95 mm threshold was used to calculate the dry days for the agriculture season since the observed daily evaporation is between 5 mm/day to 8 mm/day.

It should also be noted that a dry spell is defined as at least one day with precipitation below the selected threshold. However, for some applications, it might be desirable to redefine this. For instance, Cook *et al.* [65] used a five-day consecutive period with precipitation below predefined threshold to define the dry spell.

This study relies on a single RCM driven by a single GCM for current and future periods. Multi-model ensembles are desirable to obtain more robust climate change signal. This will partly be fulfilled with the CORDEX project that will provide this multi-GCM, multi-RCM and multi-scenario outputs [52].

Acknowledgements

This research was funded by the Ministère du Développement Économique, de l'Innovation et de l'Exportation (MDEIE) of Quebec and the Ouranos Consortium on regional climatology and adaptation to climate change.

Conflict of Interest

State any potential conflicts of interest here or "The authors declare no conflict of interest".

References and Notes

1. Solomon, S.; Qin, D.; Manning, M.; Chen, Z.; Marquis, M.; Averyt, K.B.; Tignor, M.; Miller, H.L. *Climate Change 2007: The Physical Science Basis*; Cambridge University Press: Cambridge, UK, 2007.
2. Barron, J.; Rockström, J.; Gichuki, F.; Hatibu, N. Dry spell analysis and maize yields for two semi-arid locations in East Africa. *Agric. For. Meteorol*. **2003**, *117*, 23–37.
3. Shongwe, M.E.; Van Oldenborgh, G.J.; Van Den Hurk, B.; Van Aalst, M.K. Projected changes in mean and extreme precipitation in Africa under global warming. Part II: East Africa. *J. Clim*. **2010**, *24*, 3718–3733.
4. Barnett, D.N.; Brown, S.J.; Murphy, J.M.; Sexton, D.M.H.; Webb, M.J. Quantifying uncertainty in changes in extreme event frequency in response to doubled CO_2 using a large ensemble of GCM simulations. *Clim. Dyn*. **2006**, *26*, 489–511.
5. Dai, A. Precipitation characteristics in eighteen coupled climate models. *J. Clim*. **2006**, *19*, 4605–4630.
6. Tebaldi, C.J.; Arblaster, M.; Hayhoe, K.; Meehl, G.A. Going to the extremes: An intercomparison of model-simulated historical and future changes in extreme events. *Clim. Change* **2006**, *79*, 185–211.
7. Hudson, D.A.; Jones, R.G. *Regional Climate Model Simulations of Present-Day and Future Climates of Southern Africa*; Met Office Hadley Center, Exeter, UK, 2002.
8. Sun, Y.; Solomon, S.; Dai, A.; Portmann, R. How often does it rain? *J. Clim*. **2005**, *19*, 916–934.
9. Kundzewicz, Z.W.; Mata, L.J.; Arnell, N.; Döll, P.; Kabat, P.; Jiménez, B.; Miller, K.; Oki, T.; Sen, Z.; Shiklomanov, I. Freshwater Resources and Their Management. In *Climate Change Impacts, Adaptation and Vulnerability. Contribution of Working Group II to the Fourth Assessment Report of the Intergovernmental Panel on Climate Change*; Cambridge University Press: Cambridge, UK, 2007; pp. 173–210.

10. Sushama, L.; Khaliq, M.N.; Laprise, R. Dry spell characteristics over Canada in a changing climate as simulated by the Canadian RCM. *Glob. Planet. Change* **2010**, *74*, 1–14.
11. Gao, X.; Pal, J.S.; Giorgi, F. Projected changes in mean and extreme precipitation over the Mediterranean region from a high resolution double nested RCM simulation. *Geophys. Res. Lett.* **2006**, doi: 10.1029/2005GL024954.
12. Heinrich, G.; Gobiet, A. The future of dry and wet spells in Europe : A comprehensive study based on the ENSEMBLES regional climate models. *Int. J. Climatol.* **2012**, *32*, 1951–1970.
13. May, W. Potential future changes in the characteristics of daily precipitation in Europe simulated by the HIRHAM regional climate model. *Clim. Dyn.* **2008**, *30*, 581–603.
14. Sanchez, E.; Dominguez, M.; Romera, R.; Lopez De la Franca, N.; Gaertner, M.A.; Gallardo, C.; Castro, M. Regional modeling of dry spells over the Iberian Peninsula for present climate and climate change conditions. *Clim. Change* **2011**, *107*, 625–634.
15. Hulme, M.; Doherty, R.; Ngara, T.; New, M.; Lister, D.. African climate change: 1900–2100. *Clim. Res*. **2001,** *17*, 145–168.
16. Sun, L.; Semazzi, F.H.M.; Giorgi, F.; Ogallo, L. Application of the NCAR regional climate model to eastern Africa. 1. Simulation of the short rains of 1988. *J. Geophys. Res.* **1999**, *104*, 6529–6548.
17. Sun, L.; Semazzi, F.H.M.; Giorgi, F.; Ogallo, L. Application of the NCAR regional climate model to eastern Africa. 2. Simulation of interannual variability of short rains. *J. Geophys. Res.* **1999**, *104*, 6549–6562.
18. Patricola, C. M.; Cook, K.H. Dynamics of the West African monsoon under mid-holocene precessional forcing: Regional climate model simulations. *J. Clim.* **2006**, *20*, 694–716.
19. Ibrahim, B.; Polcher, J.; Karambiri, H.; Rockel, B. Characterization of the rainy season in Burkina Faso and its representation by regional climate models. *Clim. Dyn.* **2012**, *39*, 1287–1302.
20. Joubert, A.M.; Katzfey, J.J.; McGregor, J.L.; Nguyen, K.C. Simulating midsummer climate over southern Africa using a nested regional climate model. *J. Geophys. Res.* **1999**, *104*, 19015–19025.
21. Hudson, D.A.; Jones, R.G. *Simulations of Present-day and Future Climate over Southern Africa Using HadAM3H*; Met Office Hadley Center, Exeter, UK, 2002.
22. Hewitson, B. Developing perturbations for climate change impact assessments. *EOS Trans. AGU* **2003**, *84*, 337–339.
23. Anyah, R.O.; Qiu, W. Characteristic 20th and 21st century precipitation and temperature patterns and changes over the Greater Horn of Africa. *Int. J. Climatol*. **2011**, *32*, 347–363.
24. Redelsperger J.-L.; Thorncroft, C.D.; Lebel, T.; Douglas, J.P.; Polcher, J. African monsoon multidisciplinary analysis: An international research project and field campaign. *Bull. Am. Meteorol. Soc.* **2006**, *87*, 1739–1746.
25. Sultan, B.; Janicot, S. La variabilité climatique en Afrique de l'Ouest aux échelles intra-saisonnières. I : mise en place de la mousson et variabilité intra-saisonnière de la convection. *Sécheresse* **2004**, *15*, 321–30.
26. Van der Linden, P.; Mitchell, J.F.B. *ENSEMBLES: Climate Change and its Impacts: Summary of Research and Results from the ENSEMBLES Project*; Met Office Hadley Centre, Exeter, UK, 2009.

27. Xue, Y.; De Sales, F.; Lau, W.K.M.; Boone, A.; Feng, J.; Dirmeyer, P.; Guo, Z.; Kim, K.-M.; Kitoh, A.; Kumar, V.; *et al*. Intercomparison and analyses of the climatology of the West African monsoon in the West African Monsoon Modeling and Evaluation project (WAMME) first model intercomparison experiment. *Clim. Dyn.* **2010**, *35*, 3–27.
28. Druyan, L.M.; Feng, J.; Cook, K.H.; Xue, Y.; Fulakeza, M.; Hagos, S.M.; Konaré, A.; Moufouma-Okia, W.; Rowell, D.P.; Vizy, E.K.; *et al*. The WAMME regional model intercompariason study. *Clim. Dyn.* **2010**, *35*, 175–192.
29. Giorgi, F.; Jones, C.; Asrar, G. Addressing climate information needs at the regional level: The CORDEX framework. *WMO Bull.* **2009**, *58*, 175–183.
30. Hernández-Díaz, L.; Laprise, R.; Sushama, L.; Martynov, A.; Winger, K.; Dugas, B. Climate simulation over CORDEX Africa domain using the fifth-generation Canadian Regional Climate Model (CRCM5). *Clim. Dyn*. **2013**, *40*, 1415–1433.
31. Laprise, R.; Hernandez-Diaz, L.; Tete, K.; Sushama, L.; Separovic, L.; Martynov, A.; Winger, K.; Valin, M. Climate projections over CORDEX Africa domain using the fifth-generation Canadian Regional Climate Model. *Clim. Dyn.* **2013***,* doi: 10.1007/s00382-012-1651-2.
32. Meinshausen, M.; Smith, S.J.; Calvin, K.; Daniel, J.S.; Kainuma, M.L.T.; Lamarque, J.-F.; Matsumoto, K.; Montzka, S.A.; Raper, S.C.B.; Riahi, K.; *et al*. The RCP greenhouse gas concentrations and their extensions from 1765 to 2300. *Clim. Change* **2011**, doi: 10.1007/s10584-011-0156-z.
33. Zadra, A.; Caya, D.; Cote, J.; Dugas, B.; Jones, C.; Laprise, R.; Winger, K.; Caron, L-P. The next canadian regional climate model. *Phys. Can.* **2008**, *64,* 75–83.
34. Côté, J.; Gravel, S.; Méthot, A.; Patoine, A.; Roch, M.; Staniforth, A. The operational CMC–MRB Global Environmental Multiscale (GEM) model. Part I: Design considerations and formulation. *Mon. Weather Rev.* **1998**, *126*, 1373–1395.
35. Côté, J.; Desmarais, J.-G.; Gravel, S.; Méthot, A.; Patoine, A.; Roch, M.; Staniforth, A.; The operational CMC–MRB Global Environmental Multiscale (GEM) model. Part II: Results. *Mon. Weather Rev.* **1998**, *126*, 1397–1418.
36. Yeh, K.; Côté, J.; Gravel, S.; Méthot, A.; Patoine, A.; Roch, M.; Staniforth, A. The CMC–MRB Global Environmental Multiscale (GEM) model. Part III: Nonhydrostatic formulation. *Mon. Weather Rev.* **2002**, *130*, 339–356.
37. Laprise, R. The EULER equations of motion with hydrostatic pressure as an independent variable. *Mon. Weather Rev.* **1992**, *120*, 197–207.
38. Kain, J.S.; Fritsch, J.M. A one-dimensional entraining/detraining plume model and its application in convective parameterization. *J. Atmos. Sci.* **1990**, 47, 2784–2802.
39. Kuo, H.L. On formation and intensification of tropical cyclone through latent heat release by cumulus convection. *J. Atmos Sci*, **1965**, *22*, 40–63.
40. Bélair, S.; Mailhot, J.; Girard, C.; Vaillancourt, P. Boundary-layer and shallow cumulus clouds in a medium-range forecast of a large-scale weather system. *Mon. Wea. Rev.* **2005**, *133*, 1938–1960.
41. Sundqvist, H.; Berge, E.; Kristjansson, J.E. Condensation and cloud parameterization studies with a Mesoscale numerical weather prediction model. *Mon. Wea. Rev*. **1989**, *117*, 1641–1657.
42. Li, J.; Barker, H.W. A radiation algorithm with correlated-k distribution. Part I: Local thermal equilibrium. *J. Atmos. Sci.* **2005**, *62*, 286–309.

43. McFarlane, N.A. The effect of orographically excited gravity wave drag on the general circulation of the lower stratosphere and troposphere. *J. Atmos. Sci.* **1987**, *44*, 1775–1800.
44. Zadra, A.; Roch, M.; Laroche, S.; Charron, M. The subgrid scale orographie blocking parametrization of the GEM model. *Atmos.-Ocean* **2003**, *41*, 155–170.
45. Benoit, R.; Cote, J.; Mailhot, J. Inclusion of a TKE boundary layer parameterization in the Canadian regional finite-element model. *Mon. Wea. Rev*. **1989**, *117*, 1726–1750.
46. Delage, Y.; Girard, C.; Stability functions correct at the free convection limit and consistent for both the surface and Ekman layers. *Bound. Layer Meteor*. **1992**, *58*, 19–31.
47. Delage, Y. Parameterising sub-grid scale vertical transport in atmospheric models under statically stable conditions. *Bound.-Layer Meteor*. **1997**, *82*, 23–48.
48. Verseghy, L.D. The Canadian Land Surface Scheme (CLASS): Its history and future. *Atmos. Ocean* **2000**, *38*, 1–13.
49. Simmons, A.S.; Uppala, D.D.; Kobayashi, S. ERA-interim: new ECMWF reanalysis products from 1989 onwards. *ECMWF Newsl.* **2007**, *110*, 29–35.
50. Uppala, S.; Dee, D.; Kobayashi, S.; Berrisford, P.; Simmons, A. Towards a climate data assimilation system: status update of ERA-interim. *ECMWF Newsl*. **2008**, *115*, 12–18.
51. Huffman, G.J.; Adler, R.F.; Morrissey, M.M.; Curtis, S.; Joyce, R.; McGavock, B.; Susskind, J. Global precipitation at one-degree daily resolution from multisatellite observations. *J. Hydrometeor*. **2001**, *2*, 36–50.
52. Nikulin, G.; Jones, C.; Giorgi, F.; Asrar, G.; Büchner, M.; Cerezo-Mota, R.; Christensen, O.B.; Déqué, M.; Fernandez, J.; Hänsler, A.; *et al*. Precipitation climatology in an ensemble of CORDEX-Africa regional climate simulations. *J. Clim.* **2012**, doi:10.1175/JCLI-D-11-00375.1.
53. Beniston, M.; Stephenson, D.B.; Christenson, O.B.; Ferro, C.A.T.; Frei, C.; Goyette, S.; Halsnaes, K.; Holt, T.; Jylhä, K.; Koffi, B.; *et al*. Future extreme events in European climate: an exploration of regional climate model projections. *Clim. Change* **2007**, *81*, 71–95.
54. Lana, X.; Martínez, M.D.; Burgueño, A.; Serra, C. Statistical distribution and sampling strategies for the analysis of extreme dry spells in Catalonia (NE Spain). *J. Hydrol.* **2006**, doi:10.1016/j.jhydrol.2005.09.013.
55. She, D.; Xia, J.; Song, J.; Du, H.; Chen, J.; Wan, L.; Spatio-temporal variation and statistical characteristic of extreme dry spell in Yellow River, China. *Theor. Appl. Climatol*. **2012**, doi: 10.1007/s00704-012-0731-x
56. Coles S. *An Introduction to Statistical Modeling of Extreme Values*; Springer: New York, NY, USA, 2001.
57. Christensen, J.H.; Machenhauer, B.; Jones, R.G.; Schär, C.; Ruti, P.M.; Castro, M.; Visconti, G. Validation of present regional climate simulations over Europe: LAM simulations with observed boundary conditions. *Clim. Dyn*. **1997**, 13, 489–506.
58. Walpole, R.E.; Myers, R.H. *Probability and Statistics for Engineers and Scientists*, 3rd ed.; Macmillan: New York, USA, 1985.
59. Efron, B.; Tibshirani R.J. *An Introduction to the Bootstrap. Monographs on Statistics and Applied Probability*; Chapman and Hall: New York, USA, 1993.
60. GREPHYS. Inter-comparison of regional flood frequency procedure for Canadian rivers. *J. Hydrol*. **1996**, *186*, 85–103.

61. Khaliq, M.N.; Ouarda, T.B.M.J.; Gachon, P.; Sushama, L.; St-Hilaire, A. Identification of hydrological trends in the presence of serial and cross correlations: a review of selected methods and their application to annual flow regimes of Canadian rivers. *J. Hydrol*. **2009**, *368*, 117–130.
62. Rodell, M.; Houser, P.R.; Jambor, U.; Gottschalck, J.; Mitchell, K.; Meng, C-J.; Arsenault, K.; Cosgrove, B.; Radakovich, J.; Bosilovich, M.; *et al*. The global land data assimilation system. *Bull. Amer. Meteor. Soc*. **2004**, *85*, 381–394.
63. Taylor, C.M.; Parker, D.J.; Kalthoff, N.; Gaertner, M.A.; Philippon, N.; Bastin, S.; Harris, P.P.; Boone, A.; Guichard, F.; Agustin-Panareda, A. *et al*. New perspectives on land-atmosphere feedbacks from the African monsoon multidisciplinary analysis. *Atmos. Sci. Lett.* **2011**, *12*, 38–44.
64. Mupangwa, W.; Walker, S.; Twomlow, S. Start, end and dry spells of the growing season in semi-arid southern Zimbabwe. *J. Arid Environ* **2011**, *75*, 1097–1104.
65. Cook, C.; Reason, C.J.C.; Hewitson, B.C. Wet and dry spells within particularly wet and dry summers in the South African summer rainfall region. *Clim. Res.* **2004**, *26*, 17–31.